Increase of critical current density in FeSe superconductor by strain effect

Han Luo,¹ Xinyue Wang,¹ Xin Zhou,¹ Longfei Sun,¹ Mengqin Liu,¹ Ran Guo,¹ Sheng Li,¹ Yue Sun,¹,* and Zhixiang Shi¹, †

¹ School of Physics, Southeast University, Nanjing 211189, China

Conventional J_c -enhancement methods like doping and irradiation often introduce extrinsic elements or defects, altering intrinsic properties. Here, we report a significant J_c enhancement in FeSe single crystals through compressive strain applied using a glass-fiber-reinforced plastic substrate with anisotropic thermal contraction during cooling. Under zero field at 2 K, J_c increases by a factor of \sim 4 from $\sim 2.3 \times 10^4$ to $\sim 8.7 \times 10^4$ A cm⁻²; at 5 T, it achieves an order-of-magnitude enhancement, rising from $\sim 1.0 \times 10^3$ to $\sim 1.0 \times 10^4$ A cm⁻². Analysis based on the Dew-Hughes model of the $f_p(h)$ relationship shows that strain strengthens vortex pinning, and shifts the pinning mechanism from point-like pinning to combined point and surface pinnings. This work offers an effective method to enhance FeSe's current-carrying limitation, deepens understanding of iron-based superconductors' pinning mechanisms, and highlights strain engineering's potential for optimizing superconducting performance.

I. INTRODUCTION

The critical current density J_c , which represents the upper limit of a superconductor's zero-resistance currentcarrying capacity, directly determines the performance boundaries in applications such as high-field magnets and power transmission [1–3]. A high J_c enables superconducting materials to transport larger currents, making it essential for superconducting power transmission systems, superconducting magnets, and superconducting electronic devices [4, 5]. However, the widespread application of superconductors is critically hampered by limitations in simultaneously achieving high J_c and other essential properties in practical materials. While copper oxide superconductors currently hold the record for the highest J_c values, their strong anisotropy, a small critical grain boundary angle θ_b , and high manufacturing costs pose significant challenges for industrial applications [1, 3]. In contrast, iron-based superconductors, combining a high upper critical field with low anisotropy [3, 6–13], are promising for high-field magnets and lossfree power transmission.

FeSe, the structurally simplest parent of the iron-based family [14, 15], possesses a layered lattice that exhibits a superconducting transition at 9 K under ambient pressure without chemical doping [16]. Its easy cleavability and low toxicity render FeSe an ideal platform for investigations of vortex dynamics [17], where understanding and controlling flux pinning is paramount to achieving high J_c . Nevertheless, the intrinsic critical current density of FeSe single crystals remains only $\sim 2.3 \times 10^4 \,\mathrm{A\,cm^{-2}}$ at 2 K under self-field [14, 15, 18–20], far below the practical threshold and thus constituting a key limiting factor for applications. Previous attempts to enhance J_c via chemical intercalation, aliovalent doping, or ion irradiation have indeed achieved substantial improvements. For

Here, we report the strain-engineered enhancement of J_c in FeSe. By exploiting the anisotropic thermal contraction of a glass-fiber-reinforced plastic substrate (GFRP) during cooling, compressive strain is applied to FeSe single crystals. Measurements reveal that applied strain induces a pronounced enhancement in the J_c , yielding an approximately fourfold increase at zero field, and an order-of-magnitude enhancement under a 5 T magnetic field. The pinning mechanism transforms from normal point pinning to a coexistence of normal point and surface pinning following strain application. This substrate-mediated strain-engineering strategy not only offers an effective route to surpass the currentcarrying limiting factor of FeSe, but also highlights the universal potential of strain control for optimizing superconducting performance.

II. EXPERIMENTAL DETAILS

Pristine FeSe single crystals were obtained by the chemical vapor transport growth [15, 21, 22]. To apply strain, a FeSe single crystal $(1087 \times 1048 \times 75 \,\mu\text{m}^3)$

example, sulfur doping introduces point-pinning center, and elevates J_c from $\sim 4 \times 10^4 \,\mathrm{A} \,\mathrm{cm}^{-2}$ to $\sim 6 \times 10^4 \,\mathrm{A}$ ${\rm cm^{-2}}$ at 4 K [19]. Similarly, H^+ irradiation introduces extra point pinning centers in FeSe single crystals, increasing the J_c from $\sim 3 \times 10^4$ to $\sim 8 \times 10^4$ A cm⁻² under zero field, which is an enhancement of over two times [20]. Uranium irradiation generates c-axis-aligned columnar defects, raising J_c at 2 K from 4×10^4 A cm⁻² to $2 \times 10^5 \,\mathrm{A \ cm^{-2}}$ and shifting the dominant vortex pinning mechanism from δT_c pinning to δl pinning [14]. Critically, a common drawback of these approaches is the inevitable introduction of extrinsic elements or radiationinduced defects, which usually suppresses the value of T_c and alters the stoichiometry and electronic structure. Consequently, achieving substantial J_c enhancement in FeSe via physical methods under ambient pressure remains a fundamental challenge.

 $^{^{\}ast}$ Corresponding author: sunyue@seu.edu.cn

[†] Corresponding author: zxshi@seu.edu.cn

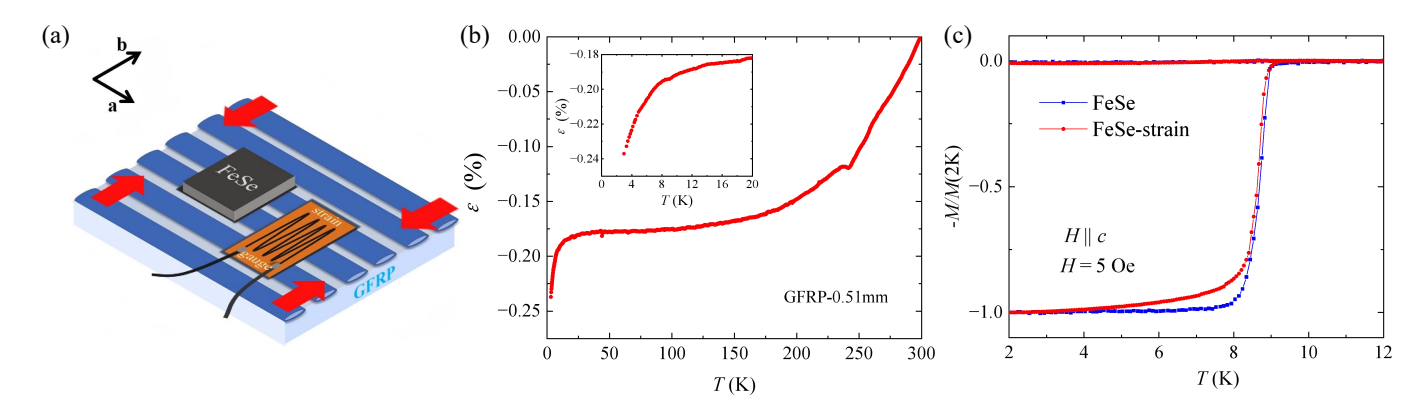


FIG. 1. (a) Schematic illustration of the contraction of the GFRP substrate and the strain measurement setup. The FeSe sample and the strain gauge were bonded using epoxy resin, with the tetragonal [100] direction of the FeSe crystal oriented parallel to the fibers of the GFRP substrate, and the sensitive grid of the strain gauge oriented perpendicular to the fibers. During the cooling process, the GFRP substrate contracts in the direction indicated by the red arrow. (b) Strain values of the 0.51 mm thick GFRP substrate as a function of temperature. The inset shows an enlarged view of the strain from 0 to 20 K. (c) Temperature dependence of the ZFC and FC magnetization of FeSe and FeSe-strain single crystals.

was cleaved and then glued onto a glass-fiber-reinforced plastic (GFRP) substrate $(3730 \times 1826 \times 466 \,\mu\text{m}^3)$ using epoxy (STYCAST 2850 FT BK 0.5 K, with Catalyst 24 LV), ensuring that the tetragonal [100] direction of the crystal was made perpendicular to the fiber direction. GFRP consists of two main components: glass fibers, which provide strength and support; synthetic resin, which acts as a binder to hold the fibers together. During the cooling process, the GFRP substrate contracts more in the direction perpendicular to the fibers than in the parallel direction [23]. To effectively transfer the compressive strain to FeSe, the epoxy resin was thinly and evenly applied to the FeSe. To accurately determine the magnitude of the compressive strain applied to the FeSe crystal along the tetragonal [010] direction, an insitu calibration was conducted using a standard resistive strain gauge (CFLA-1-350-11-6LTA-F). The strain gauge was firmly bonded to the same GFRP substrate as the FeSe crystal, following the identical epoxy bonding procedure. This combined substrate-strain-gauge assembly was installed in a Physical Property Measurement System (PPMS-9T) and underwent the same temperaturecycling protocol as that used in the superconducting measurements. The non-magnetic property of GFRP makes it suitable for magnetic measurements [24]. Magnetic measurements were performed using the Magnetic Property Measurement System (MPMS-XL5, Quantum Design). The magnetic field sweep rate was set to $120 \,\mathrm{Oe}\,\mathrm{s}^{-1}$ for magnetic hysteresis loops (MHLs).

III. RESULTS AND DISCUSSION

Fig. 1(a) illustrates the experimental setup designed to transmit compressive strain to the FeSe crystal. The crystal and a resistive strain gauge were bonded to the GFRP substrate using epoxy resin. The tetragonal [100]

direction of the FeSe crystal was aligned parallel to the substrate's fibers, while the sensitive grid of the strain gauge was oriented perpendicular to them. During cooling, the GFRP substrate contracts predominantly along the direction indicated by the red arrow. In this configuration, a strain gauge is a sensor that converts the deformation of a material into changes in resistance [25–27]. In the context of iron-based superconductors, strain gauges have been widely employed to characterize anisotropic strain, particularly in studies of electronic nematicity and structural transitions [28–30]. For instance, in FeSe and related compounds, strain gauges have been used to measure the transmission efficiency of strain from substrates to crystals [31]. To measure the strain experienced by FeSe due to the contraction of 0.51 mm-thick GFRP at low temperatures, a resistive strain gauge was employed. As the temperature decreases, the GFRP contracts in the direction perpendicular to the fibers, causing the sensitive grid of the strain gauge attached to it to deform. This deformation leads to a change in the resistance of the strain gauge. The change in resistance is proportional to the strain ϵ via $\Delta R/R = K\epsilon$, where K is the gauge factor of the strain gauge. This relationship allows for the determination of the strain value. Fig. 1(b) shows the strain of the 0.51 mm-thick GFRP as a function of temperature. As the temperature decreases, the contraction of the GFRP increases. It contracts rapidly during the cooling process down to 250 K. Below 250 K, the contraction rate becomes relatively slower. The fastest contraction occurs when the temperature drops from 10 K to 3 K. At 3 K, the strain in the GFRP is approximately -0.24%.

Fig. 1(c) illustrates the temperature dependence of field cooling (FC) and zero FC (ZFC) magnetization at 5 Oe for FeSe and FeSe-strain single crystals. The superconducting transition temperature $T_{\rm c}$ of FeSe-strain remains essentially unchanged at 9 K, comparable to that of

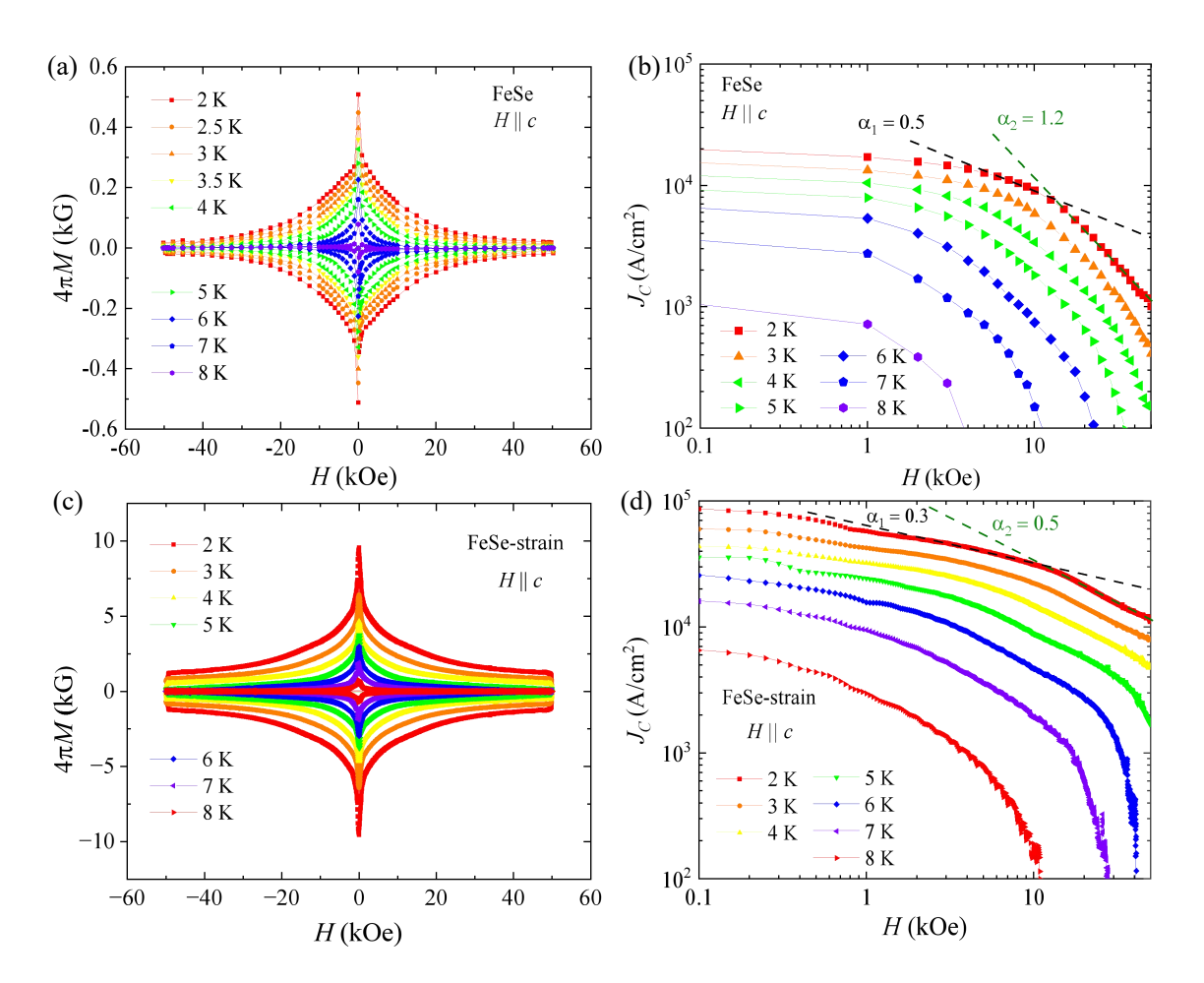


FIG. 2. The temperature dependence of MHLs for H||c| and the magnetic field dependence of the J_c derived from the Bean model. (a) and (b) correspond to FeSe, while (c) and (d) correspond to FeSe-strain. In panels (b) and (d), the dashed lines represent the exponent α obtained from fitting the critical current density to the power-law relation $J_c \propto H^{-\alpha}$. The black dashed line indicates the exponent in the range of $5-10\,\mathrm{kOe}$, while the green dashed line corresponds to the exponent above $10\,\mathrm{kOe}$.

pristine FeSe. This result demonstrates that the strain effect has no influence on the T_c of FeSe. Hydrostatic pressure has a significant effect on the T_c of FeSe [32]. This is because under hydrostatic pressure, the FeSe lattice is uniformly compressed, which alters the band structure and enhances spin fluctuations, thus significantly increasing T_c [33]. In contrast, the compressive strain is applied in the ab plane and mainly tunes the nematicity and the associated orbital degrees of freedom. Its effect on the overall Fermi-surface volume and the enhancement of spin fluctuations is limited. For instance, as demonstrated in a recent study on FeSe under in-plane uniaxial strain along the [110] direction, a compressive strain of about 0.2% induces only a minimal shift in T_c of approximately 0.2 K [34].

In Fig. 2(a), the MHLs of FeSe and FeSe-strain at different temperatures are measured and compared. The MHLs for both crystals are nearly symmetric, reflecting the dominance of bulk pinning. Unlike many other iron-based superconductors [35–39], these loops show no evidence of a second magnetization peak, and M displays

a monotonic decrease with increasing H. By selecting appropriate normalization parameters M and H, MHLs measured at different temperatures can be normalized onto a single curve if one pinning mechanism is dominant [40-43]. When multiple pinning mechanisms coexist, the normalized curves will not overlap, thereby intuitively reflecting the variation in pinning mechanisms. The maximum magnetization value (M^*) are selected and the irreversibility field (H^*) is determined by extrapolating J_c to zero in the $J_c^{1/2}$ -H curve [14, 15, 44]. As shown in Figs. 3(a) and 3(b), the normalized MHLs for FeSe measured at different temperatures scaled well, indicating that the FeSe crystal is dominated by a single pinning mechanism. In contrast, the normalized MHLs for FeSestrain are altered and do not fully overlap across temperatures. Fig. 3(c) compares the scaling MHLs of FeSe and FeSe-strain at 5 K. The difference is due to the variation in pinning mechanisms caused by the application of compressive strain, which will be discussed in detail

The critical current density $J_{\rm c}$ can be extracted from

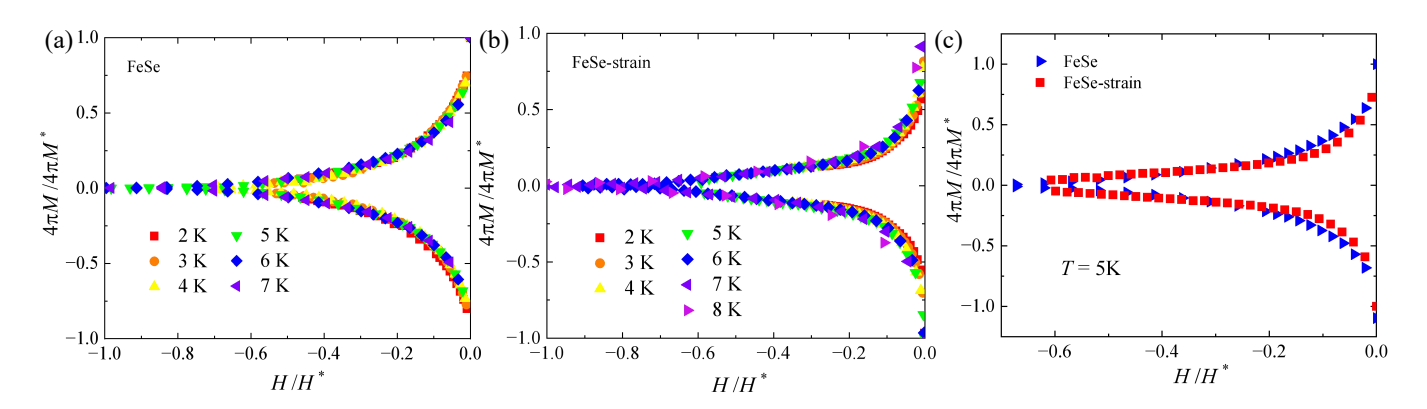


FIG. 3. Scaled MHLs for (a) FeSe and (b) FeSe-strain, respectively, at different temperatures. (c) Scaled MHLs at 5 K for the pristine and strained crystals.

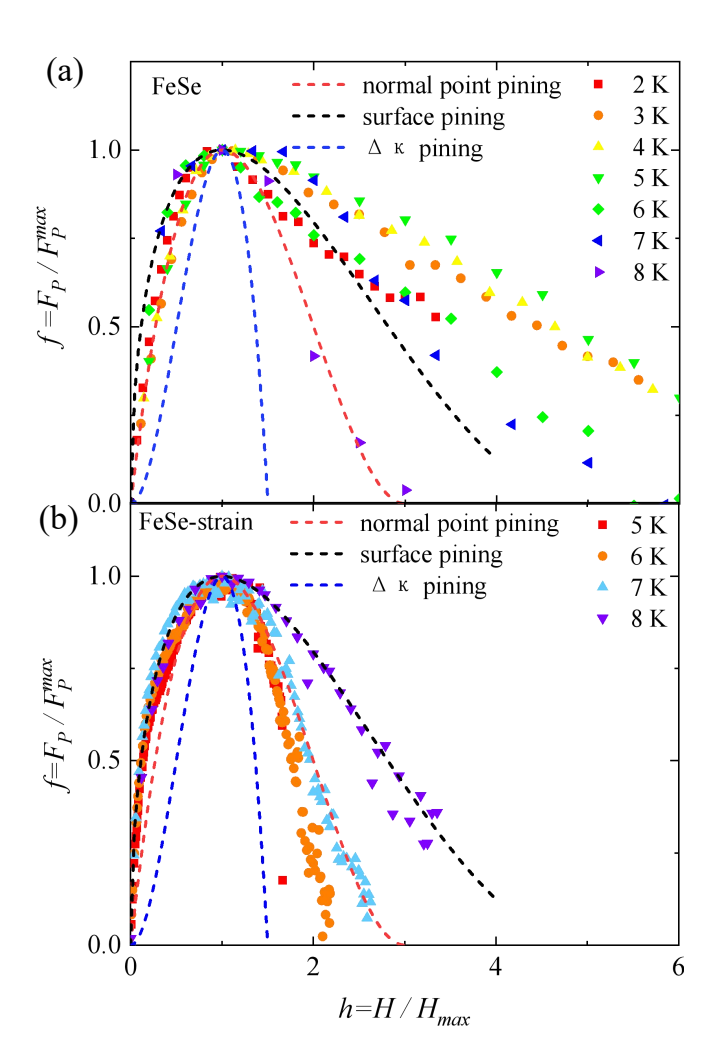


FIG. 4. The temperature variation of the normalized vortex pinning force $(f = F_{\rm p}/F_{\rm pmax})$ and reduced field $(h = H/H_{\rm max})$ for FeSe and FeSe-strain.

the MHLs using the extended Bean model [45], which is

given by:

$$J_{\rm c} = \frac{20\Delta M}{a(1 - a/3b)}.$$

Here, ΔM (emu cm⁻³) denotes the difference between the magnetization during the upward and downward field sweeps, while a and b dcorrespond to the width and length of the crystals, respectively. It should be noted that the pre-factor 20 in this expression is dimensionless when consistent magnetic units are employed, as emphasized in recent work on unit conversion in Bean's model [46]. Figs. 2(b) and 2(d) present the J_c of FeSe and FeSestrain at various temperatures. At zero field and 2 K, the J_c of pristine FeSe is $\sim 2.3 \times 10^4$ A cm⁻². With increasing the magnetic field to 5 T, J_c decreases to 1.0×10^3 A cm⁻². At zero field, the J_c of FeSe-strain reaches approximately 8.7×10^4 A cm⁻², representing an approximately fourfold increase compared to its unstrained state. Under a 5 T magnetic field, the J_c of FeSe-strain is 1.0×10^4 A cm⁻², an enhancement by one order of magnitude over that of unstrained FeSe single crystals. This substantial improvement in J_c at high fields originates from straininduced strengthening of flux pinning, enabling FeSe to retain a significantly higher dissipation-free current capacity under these conditions. Collectively, these results demonstrate that the strain effect is effective in enhancing the superconducting performance of FeSe.

 J_c for both crystals exhibits minimal variation below 1 kOe. Above 5 kOe, J_c decays according to a power law, $H^{-\alpha}$. For FeSe, in the magnetic field range of 5-10 kOe, the power-law exponent α is approximately 0.5. This is attributed to the strong pinning by sparse nanometer-sized defects, similar to the case of YBCO films [47, 48]. In high magnetic fields above 10 kOe, the decay rate of J_c significantly increases to $\alpha \sim 1.2$. Since the pinning force $F_p = \mu_0 H \cdot J_c$, the fact that F_p remains constant implies that J_c decreases proportionally to H^{-1} with increasing magnetic field [49]. In FeSe, high magnetic fields cause the limited strong pinning centers to become fully occupied by flux lines. This saturation of the pinning force results in a rapid suppression of J_c , which conse-

quently exhibits an inverse proportionality to H. In contrast, FeSe-strain shows a more gradual decay in the 5-10 kOe magnetic field range, with a power-law exponent $\alpha \sim 0.3$. Computational studies employing large-scale time-dependent Ginzburg-Landau theory have demonstrated that it is due to the pinning from spherical defects [50–53]. Above 10 kOe, the power-law exponent α for FeSe-strain remains at 0.5, significantly lower than the $\alpha \sim 1.2$ observed for FeSe, indicating that strain creates a new pinning center. After applying strain, the field dependence of J_c is modified. The power-law exponent shifts from $H^{-0.5}$ to $H^{-0.3}$ at low magnetic fields. Similarly, the field dependence of J_c undergoes pronounced attenuation at high magnetic fields, reducing from $H^{-1.2}$ to $H^{-0.5}$. Strain effectively maintains the binding ability of pinning centers on vortex lines, suppressing the weakening of pinning barriers due to vortex-vortex interactions at high magnetic fields, thereby avoiding a sharp drop in J_c .

Various experimental methods have been proven to effectively enhance the J_c of FeSe. For instance, sulfur (S) doping-induced lattice distortion can reduce the size of magnetic flux bundles and increase effective pinning energy. In the $FeSe_{0.86}S_{0.14}$ single crystals, the J_c at 2 K and self-field increases to approximately 6×10^4 A cm⁻², compared with the J_c of about 4×10^4 A cm⁻² in the original FeSe single crystals [19]. Ion irradiation is another approach that can be employed to enhance the J_c of FeSe. By appropriately selecting ion types and energies for irradiation, various defects can be introduced into superconducting materials, which in turn enables the control of pinning defects. For instance, point defects were successfully introduced into FeSe single crystals through 3 MeV H^+ irradiation [20]. Consequently, the J_c increased to approximately $8 \times 10^4 \,\mathrm{A \ cm^{-2}}$, more than doubling the original value. Furthermore, uranium irradiation can introduce columnar defects along the c axis in FeSe single crystals [14]. As a result, the J_c at 2 K was enhanced to $2 \times 10^5 \,\mathrm{A \, cm^{-2}}$, which is more than five times higher than the original $4 \times 10^4 \,\mathrm{A} \,\mathrm{cm}^{-2}$. Compared with the situation where T_c drops dramatically from 9.2 K to 5 K after irradiation by uranium with $B_{\Phi} = 16 \,\mathrm{T}$, strain tuning achieves a significant increase in J_c while maintaining T_c almost unchanged, providing a new approach for optimizing the performance of FeSe superconducting materials.

To achieve a more thorough comprehension of the vortex pinning mechanism, Figs. 4(a) and 4(b) display the temperature dependence of the normalized vortex pinning force ($f = F_{\rm p}/F_{\rm pmax}$) and reduced field ($h = H/H_{\rm max}$) for FeSe and FeSe-strain. Here, $H_{\rm max}$ indicates the magnetic field peak, whereas $F_{\rm pmax}$ represents the maximum pinning force. The $F_{\rm p}$ determines the motion and positioning of vortices in a magnetic field, and it was calculated using $F_{\rm p} = \mu_0 H \times J_{\rm c}$. Within the Dew-Hughes model [54], there is a specific functional relationship between f and h, given by $f_{\rm p} \propto h_{\rm p} (1-h)^q$, where the parameters p and q are determined by the pinning mechanism. The main pinning mechanism includes

 $\Delta \kappa$ pinning, normal point pinning, and surface pinning. Within a particular temperature range, if h meets any of the following equations, it shows that the corresponding pinning mechanism is dominant.

$$f_{\rm p} = \frac{9}{4}h(1 - h/3)^2$$
 for normal point pinning, (1)

$$f_{\rm p} = \frac{25}{16} h^{1/2} (1 - h/5)^2$$
 for surface pinning, (2)

$$f_{\rm p} = 3h^2(1 - 2h/3)$$
 for $\Delta \kappa$ pinning. (3)

For high- T_c superconductors, flux creep is highly pronounced, particularly under high fields, and exhibits both temperature and field dependence. Consequently, the pinning force F_p usually cannot be scaled at high fields, as has been observed in cuprates [55–57] and in several iron-based superconductors (IBSs) [58, 59]. Although the T_c of FeSe is relatively low, its flux-creep rate is comparable to that of other high- T_c superconductors [15, 60]. Owing to this failure of scaling at high fields, such data cannot be directly compared with the theoretical models [61, 62]. Therefore, the analysis is restricted to the lowfield regime (h < 1), where flux creep has minimal influence. In this regime, the scaled data for pristine FeSe can be reasonably fitted by the normal point-pinning model, as shown in Fig. 4(a). In contrast, the strained FeSe data lie between the theoretical curves for normal point pinning and surface pinning. These results are further supported by the slope change observed in the field dependence of J_c , as shown in Fig. 2.

In pristine FeSe, $f_{\rm P}$ between 2-6 K can be well fitted with equation (1), indicating that normal point pinning is the dominant pinning mechanism. The pinning centers for normal point pinning are located within the superconductor, such as at impurities or defects, around which flux lines distribute, and the J_c of the superconductor is mainly influenced by these internal pinning centers. For FeSe-strain, between $2-4\,\mathrm{K}$, the $F_{\mathrm{P}}-H$ curves diverge, making it hard to determine F_{pmax} [63]. Hence, Fig. 3(b) presents the f-h results at 5-8 K. Within 5-8 K, the $f_{\rm P}$ pinning mechanism of FeSe-strain exhibits intermediate characteristics between normal point pinning and surface pinning, suggesting the coexistence of both pinning centers. Normal point pinning refers to the internal pinning centers' dominant role in flux line pinning, while the surface pinning implies the surface or interface-related pinning is dominant. This transition in pinning mechanism reveals the physical origin underlying the previously observed reduction in the power-law exponent α of $J_{\rm c} \propto H^{-\alpha}$. Specifically, the enhanced surface pinning induces a significant decrease in α from ~ 1.2 to ~ 0.5 . Future studies could employ high-resolution transmission electron microscopy (HRTEM) and scanning tunneling microscopy (STM) to directly investigate the types and spatial distribution of defects introduced in strained FeSe crystals. This approach would help clarify the intrinsic nature of strain-induced pinning centers and elucidate the mechanisms underlying their enhanced vortex-pinning capability.

IV. CONCLUSION

In summary, compressive strain was applied to FeSe single crystals using an anisotropically contracting GFRP substrate. While the T_c remains unchanged, the J_c is significantly enhanced. At 2 K and zero field, J_c increases approximately fourfold, and achieves an order-of-magnitude enhancement under a 5 T magnetic field. Analysis shows that the strain reduces the decay rate of J_c , confirming the enhanced flux pinning strength. This mitigates the weakening of the pinning potential barrier by vortex interactions at high fields, preventing the sharp J_c decline. Dew-Hughes model analysis further reveals a coexistence of normal point pinning and surface pinning in FeSe-strain. These results demonstrate that strain ef-

fectively enhances flux pinning in FeSe by modifying its structural and defect characteristics, offering a promising pathway for optimizing FeSe and related iron-based superconductors.

ACKNOWLEDGMENTS

This work was partly supported by the National Key R&D Program of China (Grants No. 2024YFA1408400) and the National Natural Science Foundation of China (Grants No. 12374136, No. 12374135, No. U24A2068, No. 12204487).

H.L. and X.W. contributed equally to this work.

- [1] Dong Li, Jie Yuan, Peipei Shen, Chuanying Xi, Jinpeng Tian, Shunli Ni, Jingsong Zhang, Zhongxu Wei, Wei Hu, Zian Li, et al. Giant enhancement of critical current density at high field in superconducting (Li, Fe) OHFeSe films by mn doping. Superconductor Science and Technology, 32(12):12LT01, 2019.
- [2] Gianni Blatter, Mikhail V Feigel'man, Vadim B Geshkenbein, Anatoly I Larkin, and Valerii M Vinokur. Vortices in high-temperature superconductors. Reviews of Modern Physics, 66(4):1125, 1994.
- [3] Hideo Hosono, Akiyasu Yamamoto, Hidenori Hiramatsu, and Yanwei Ma. Recent advances in iron-based superconductors toward applications. *Materials Today*, 21(3):278– 302, 2018.
- [4] David Larbalestier, Alex Gurevich, D Matthew Feldmann, and Anatoly Polyanskii. High-T_c superconducting materials for electric power applications. *Nature*, 414(6861):368–377, 2001.
- [5] David C Larbalestier, J Jiang, U.P. Trociewitz, F Kametani, C Scheuerlein, M Dalban-Canassy, M Matras, P Chen, NC Craig, PJ Lee, et al. Isotropic round-wire multifilament cuprate superconductor for generation of magnetic fields above 30 T. Nature Materials, 13(4):375–381, 2014.
- [6] F Hunte, J Jaroszynski, A Gurevich, DC Larbalestier, Rongying Jin, AS Sefat, Michael A McGuire, Brian C Sales, David K Christen, and David Mandrus. Two-band superconductivity in LaFeAsO_{0.89}F_{0.11} at very high magnetic fields. *Nature*, 453(7197):903–905, 2008.
- [7] Philip JW Moll, Roman Puzniak, Fedor Balakirev, Krzysztof Rogacki, Janusz Karpinski, Nikolai D Zhigadlo, and Bertram Batlogg. High magnetic-field scales and critical currents in SmFeAs(O, F) crystals. *Nature Materials*, 9(8):628–633, 2010.
- [8] Takayoshi Katase, Yoshihiro Ishimaru, Akira Tsukamoto, Hidenori Hiramatsu, Toshio Kamiya, Keiichi Tanabe, and Hideo Hosono. Advantageous grain boundaries in iron pnictide superconductors. *Nature Communications*, 2(1):409, 2011.
- [9] Qiang Li, Weidong Si, and Ivo K Dimitrov. Films of iron chalcogenide superconductors. Reports on Progress in Physics, 74(12):124510, 2011.
- [10] Weidong Si, Su Jung Han, Xiaoya Shi, Steven N Ehrlich,

- J Jaroszynski, Amit Goyal, and Qiang Li. High current superconductivity in FeSe_{0.5}Te_{0.5}-coated conductors at 30 tesla. *Nature Communications*, 4(1):1347, 2013.
- [11] S Haindl, M Kidszun, S Oswald, C Hess, B Büchner, S Kölling, L Wilde, Thomas Thersleff, VV Yurchenko, M Jourdan, et al. Thin film growth of Fe-based superconductors: from fundamental properties to functional devices. a comparative review. Reports on Progress in Physics, 77(4):046502, 2014.
- [12] Xianping Zhang, Chao Yao, He Lin, Yao Cai, Zhen Chen, Jianqi Li, Chiheng Dong, Qianjun Zhang, Dongliang Wang, Yanwei Ma, et al. Realization of practical level current densities in Sr_{0.6}K_{0.4}Fe₂As₂ tape conductors for high-field applications. Applied Physics Letters, 104(20), 2014.
- [13] J Hänisch, K Iida, R Hühne, and C Tarantini. Fe-based superconducting thin films—preparation and tuning of superconducting properties. Superconductor Science and Technology, 32(9):093001, 2019.
- [14] Yue Sun, Akiyoshi Park, Sunseng Pyon, Tsuyoshi Tamegai, Tadashi Kambara, and Ataru Ichinose. Effects of heavy-ion irradiation on FeSe. *Physical Review B*, 95(10):104514, 2017.
- [15] Yue Sun, Sunseng Pyon, Tsuyoshi Tamegai, Ryo Kobayashi, Tatsuya Watashige, Shigeru Kasahara, Yuji Matsuda, and Takasada Shibauchi. Critical current density, vortex dynamics, and phase diagram of singlecrystal FeSe. *Physical Review B*, 92(14):144509, 2015.
- [16] TM McQueen, AJ Williams, PW Stephens, J Tao, Y Zhu, V Ksenofontov, F Casper, C Felser, and RJ Cava. Tetragonal-to-orthorhombic structural phase transition at 90 k in the superconductor Fe_{1.01}Se. *Physical Review Letters*, 103(5):057002, 2009.
- [17] Taichi Terashima, Hideaki Fujii, Yoshitaka Matsushita, Shinya Uji, Yuji Matsuda, Takasada Shibauchi, and Shigeru Kasahara. Transport evidence for twin-boundary pinning of superconducting vortices in FeSe. *Physical Review B*, 109(1):014518, 2024.
- [18] Yan Meng, Wei Wei, Xiangzhuo Xing, Xiaolei Yi, Nan Zhou, Yufeng Zhang, Wenhui Liu, Yue Sun, and Zhixiang Shi. Significant enhancement of critical current density in H+-intercalated FeSe single crystal. Superconductor Science and Technology, 35(7):075012, 2022.

- [19] Yue Sun, Sunseng Pyon, and Tsuyoshi Tamegai. Effect of S doping on the critical current density and vortex dynamics in FeSe single crystal. *Physica C: Supercon*ductivity and its Applications, 530:55–57, 2016.
- [20] Yue Sun, Sunseng Pyon, Tsuyoshi Tamegai, Ryo Kobayashi, Tatsuya Watashige, Shigeru Kasahara, Yuji Matsuda, Takasada Shibauchi, and Hisashi Kitamura. Enhancement of critical current density and mechanism of vortex pinning in H+-irradiated FeSe single crystal. Applied Physics Express, 8(11):113102, 2015.
- [21] Yue Sun, Sunseng Pyon, and Tsuyoshi Tamegai. Electron carriers with possible dirac-cone-like dispersion in $\text{FeSe}_{1-x}S_x$ (x = 0 and 0.14) single crystals triggered by structural transition. *Physical Review B*, 93(10):104502, 2016.
- [22] Qiang Hou, Wei Wei, Xin Zhou, Wenhui Liu, Ke Wang, Xiangzhuo Xing, Yufeng Zhang, Nan Zhou, Yongqiang Pan, Yue Sun, et al. Bulk and surface Dirac states accompanied by two superconducting domes in FeSe-based superconductors. Proceedings of the National Academy of Sciences, 121(48):e2409756121, 2024.
- [23] Mingquan He, Liran Wang, Felix Ahn, Frédéric Hardy, Thomas Wolf, Peter Adelmann, Jörg Schmalian, Ilya Eremin, and Christoph Meingast. Dichotomy between inplane magnetic susceptibility and resistivity anisotropies in extremely strained BaFe₂As₂. Nature Communications, 8(1):504, 2017.
- [24] See Supplemental Material at [] for the magnetization and *M-H* curve of GFRP at 2 K, showing paramematic behavior with no hysteresis.
- [25] Ziye Mo, Chunyi Li, Wenting Zhang, Chang Liu, Yongxin Sun, Ruixian Liu, and Xingye Lu. Cryogenic Digital Image Correlation as a Probe of Strain in Iron-Based Superconductors. *Chinese Physics Letters*, 41(10):107102, 2024.
- [26] Jiun-Haw Chu, Hsueh-Hui Kuo, James G Analytis, and Ian R Fisher. Divergent nematic susceptibility in an iron arsenide superconductor. *Science*, 337(6095):710– 712, 2012.
- [27] Suguru Hosoi, Kohei Matsuura, Kousuke Ishida, Hao Wang, Yuta Mizukami, Tatsuya Watashige, Shigeru Kasahara, Yuji Matsuda, and Takasada Shibauchi. Nematic quantum critical point without magnetism in $\text{FeSe}_{1-x}\mathbf{S}_x$ superconductors. Proceedings of the National Academy of Sciences, 113(29):8139–8143, 2016.
- [28] Hsueh-Hui Kuo, Maxwell C Shapiro, Scott C Riggs, and Ian R Fisher. Measurement of the elastoresistivity coefficients of the underdoped iron arsenide Ba(Fe_{0.975}Co_{0.025})₂As₂. Physical Review B—Condensed Matter and Materials Physics, 88(8):085113, 2013.
- [29] Hsueh-Hui Kuo, Jiun-Haw Chu, Johanna C Palmstrom, Steven A Kivelson, and Ian R Fisher. Ubiquitous signatures of nematic quantum criticality in optimally doped Fe-based superconductors. *Science*, 352(6288):958–962, 2016
- [30] Johanna C Palmstrom, Alexander T Hristov, Steven A Kivelson, J-H Chu, and Ian R Fisher. Critical divergence of the symmetric (A_{1g}) nonlinear elastoresistance near the nematic transition in an iron-based superconductor. *Physical Review B*, 96(20):205133, 2017.
- [31] Makariy A Tanatar, Anna E Böhmer, Erik I Timmons, M Schütt, G Drachuck, Valentin Taufour, K Kothapalli, Andreas Kreyssig, SL Bud'ko, PC Canfield, et al. Origin of the resistivity anisotropy in the nematic phase of FeSe.

- Physical Review letters, 117(12):127001, 2016.
- [32] JP Sun, K Matsuura, GZ Ye, Y Mizukami, M Shimozawa, Kazuyuki Matsubayashi, M Yamashita, T Watashige, Shigeru Kasahara, Y Matsuda, et al. Dome-shaped magnetic order competing with high-temperature superconductivity at high pressures in FeSe. *Nature communica*tions, 7(1):12146, 2016.
- [33] Kohei Matsuura, Yuta Mizukami, Y. Arai, Y. Sugimura, N. Maejima, A. Machida, T. Watanuki, T. Fukuda, T. Yajima, Z. Hiroi, et al. Maximizing T_c by tuning nematicity and magnetism in FeSe_{1-x}S_x superconductors. Nature Communications, 8(1):1143, 2017.
- [34] Ruixian Liu, Qi Tang, Chang Liu, Wenting Zhang, Chunyi Li, Kaijuan Zhou, Qiaoyu Wang, and Xingye Lu. Evolution of pairing symmetry in FeSe_{1-x}S_x as probed by in-plane strain tuning of T_c . Physical Review B, 112(9):094514, 2025.
- [35] Ruslan Prozorov, Ni Ni, MA Tanatar, VG Kogan, RT Gordon, C Martin, EC Blomberg, P Prommapan, JQ Yan, SL Bud'ko, et al. Vortex phase diagram of Ba(Fe_{0.93}Co_{0.07})₂As₂ single crystals. *Physical Review B*, 78(22):224506, 2008.
- [36] N Haberkorn, M Miura, B Maiorov, GF Chen, W Yu, and L Civale. Strong pinning and elastic to plastic vortex crossover in Na-doped CaFe₂As₂ single crystals. *Physical Review B*, 84(9):094522, 2011.
- [37] S Salem-Sugui Jr, L Ghivelder, AD Alvarenga, LF Cohen, KA Yates, K Morrison, JL Pimentel Jr, Huiqian Luo, Zhaosheng Wang, and Hai-Hu Wen. Flux dynamics associated with the second magnetization peak in the iron pnictide Ba_{1-x}K_xFe₂As₂. Physical Review B, 82(5):054513, 2010.
- [38] Xiangzhuo Xing, Xiaolei Yi, Meng Li, Yan Meng, Gang Mu, Jun-Yi Ge, and Zhixiang Shi. Vortex phase diagram in 12442-type RbCa₂Fe₄As₄F₂ single crystal revealed by magneto-transport and magnetization measurements. Superconductor Science and Technology, 33(11):114005, 2020.
- [39] Xiangzhuo Xing, Zhanfeng Li, Ivan Veshchunov, Xiaolei Yi, Yan Meng, Meng Li, Bencheng Lin, Tsuyoshi Tamegai, and Zhixiang Shi. Reemergence of superconductivity by 4d transition-metal Pd doping in over-doped 112-type iron pnictide superconductors Ca_{0.755}La_{0.245}FeAs₂. New Journal of Physics, 21(9):093015, 2019.
- [40] GK Perkins, LF Cohen, AA Zhukov, and AD Caplin. Implications of magnetic-hysteresis-loop scaling in hightemperature superconductors. *Physical Review B*, 51(13):8513, 1995.
- [41] M Oussena, PAJ De Groot, A Marshall, and JS Abell. Magnetization scaling on thick YBa₂Cu₃O_{7-x} single crystals. *Physical Review B*, 49(2):1484, 1994.
- [42] CD Dewhurst, DA Cardwell, AM Campbell, RA Doyle, G Balakrishnan, and D McK Paul. Determination of the onset of bulk pinning and the low-temperatureirreversibility line in Bi₂Sr₂CaCu₂O_{8+δ}. Physical Review B, 53(21):14594, 1996.
- [43] CD Dewhurst, RA Doyle, G Balakrishnan, G Wirth, and D McK Paul. Separation of enhanced and residual pinning mechanisms in single-crystal $\mathrm{Bi}_2\mathrm{Sr}_2\mathrm{CaCu}_2\mathrm{O}_{8+\delta}$ irradiated with heavy ions. *Physical Review B*, 62(21):14373, 2000.
- [44] See Supplemental Material at [] for the scaling procedure of the MHLs based on the maximum magnetization (M^*)

- and the irreversibility field (H^*) .
- [45] Charles P Bean. Magnetization of High-Field Superconductors. Reviews of Modern Physics, 36(1):31–39, 1964.
- [46] Massimiliano Polichetti, Armando Galluzzi, Rohit Kumar, and Amit Goyal. Equation for Calculation of Critical Current Density Using the Bean's Model with Self-Consistent Magnetic Units to Prevent Unit Conversion Errors. *Materials*, 18(2):269, 2025.
- [47] CJ Van der Beek, M Konczykowski, A Abal'oshev, I Abal'osheva, P Gierlowski, SJ Lewandowski, MV Indenbom, and S Barbanera. Strong pinning in hightemperature superconducting films. *Physical Review B*, 66(2):024523, 2002.
- [48] CJ Van der Beek, Giancarlo Rizza, Marcin Konczykowski, Pierre Fertey, Isabelle Monnet, Thierry Klein, Ryuji Okazaki, Motoyuki Ishikado, Hijiri Kito, Akira Iyo, et al. Flux pinning in PrFeAsO_{0.9} and NdFeAsO_{0.9}F_{0.1} superconducting crystals. *Physical Re*view B, 81(17):174517, 2010.
- [49] L Krusin-Elbaum, L Civale, JR Thompson, and C Feild. Accommodation of vortices to columnar defects: Evidence for large entropic reduction of vortex localization. Physical Review B, 53(17):11744, 1996.
- [50] Akiyoshi Park, Ivan Veshchunov, Akinori Mine, Sunseng Pyon, Tsuyoshi Tamegai, and Hisashi Kitamura. Effects of 6 MeV proton irradiation on the vortex ensemble in BaFe₂(As_{0.67}P_{0.33})₂ revealed through magnetization measurements and real-space vortex imaging. *Physical Review B*, 101(22):224507, 2020.
- [51] Toshihiro Taen, Fumiaki Ohtake, Sunseng Pyon, Tsuyoshi Tamegai, and Hisashi Kitamura. Critical current density and vortex dynamics in pristine and protonirradiated Ba_{0.6}K_{0.4}Fe₂As₂. Superconductor Science and Technology, 28(8):085003, 2015.
- [52] Toshihiro Taen, Yasuyuki Nakajima, Tsuyoshi Tamegai, and Hisashi Kitamura. Enhancement of critical current density and vortex activation energy in proton-irradiated Co-doped BaFe₂As₂. Physical Review B, 86(9):094527, 2012.
- [53] Roland Willa, Alexei E Koshelev, Ivan A Sadovskyy, and Andreas Glatz. Strong-pinning regimes by spherical inclusions in anisotropic type-II superconductors. Superconductor Science and Technology, 31(1):014001, 2017.

- [54] D Dew-Hughes. Flux pinning mechanisms in type II superconductors. Philosophical Magazine, 30(2):293–305, 1974
- [55] T. Higuchi, S. I. Yoo, and M. Murakami. Comparative study of critical current densities and flux pinning among a flux-grown NdBa₂Cu₃O_y single crystal, melt-textured Nd-Ba-Cu-O, and Y-Ba-Cu-O bulks. *Phys. Rev. B*, 59(2):1514–1527, 1999.
- [56] Lior Klein, E. R. Yacoby, Y. Yeshurun, A. Erb, G. Müller-Vogt, V. Breit, and H. Wühl. Peak effect and scaling of irreversible properties in untwinned Y-Ba-Cu-O crystals. *Phys. Rev. B*, 49(6):4403–4416, 1994.
- [57] L. Civale, M. W. McElfresh, A. D. Marwick, et al. Weak links and dc SQUIDs on artificial nonsymmetric grain boundaries in YBa₂Cu₃O_{7-δ}. Phys. Rev. B, 43(13):732– 735, 1991.
- [58] Mingtao Li, La Chen, Wen-Long You, Junyi Ge, and Jincang Zhang. Giant increase of critical current density and vortex pinning in Mn doped $K_xFe_{2-y}Se_2$ single crystals. *Appl. Phys. Lett.*, 105(19):192601, 2014.
- [59] L. Fang, Y. Jia, J. A. Schlueter, A. Kayani, Z. L. Xiao, H. Claus, U. Welp, A. E. Koshelev, G. W. Crabtree, and W.-K. Kwok. Doping- and irradiation-controlled pinning of vortices in BaFe₂(As_{1-x}P_x)₂ single crystals. *Phys. Rev. B*, 84(14):140504, 2011.
- [60] Yue Sun, Toshihiro Taen, Yuji Tsuchiya, Sunseng Pyon, Zhixiang Shi, and Tsuyoshi Tamegai. Magnetic relaxation and collective vortex creep in FeTe_{0.6}Se_{0.4} single crystal. *Europhys. Lett.*, 103(5):57013, 2013.
- [61] Xiaofei Huang, Yue Sun, Yongqiang Pan, and Zhixiang Shi. Magnetization loops and non-scaling behavior of flux pinning force of Fe_{1+y}Te_{1-x}Se_x studied by numerical simulation. Supercond. Sci. Technol., 35(10):105003, 2022.
- [62] Yongqiang Pan, Nan Zhou, Bencheng Lin, Jinhua Wang, Zengwei Zhu, Wei Zhou, Yue Sun, and Zhixiang Shi. Anisotropic critical current density and flux pinning mechanism of Fe_{1+y}Te_{0.6}Se_{0.4} single crystals. Supercond. Sci. Technol., 35(1):015002, 2021.
- [63] See Supplemental Material at [] for the magnetic field dependence of the pinning F_p for the FeSe-strain crystal.